Original Article

JOURNAL OF REINFORCED PLASTICS & COMPOSITES

Journal of Reinforced Plastics and Composites
2014, Vol 33(11) 1048–1058

DOI: 10.1177/0731684414523060
jrp.sagepub.com

SAGE

Applied research of stainless steel fiber-filled acrylonitrile–butadiene–styrene copolymer composites

Xian-nan Luo[1], Xiang Fang[1], Ke-gang Wu[2], Zhi-yang Chen[2], Tian-tian Guo[2] and Qing-tao Wang[2]

Abstract

Composite is prepared by filling acrylonitrile–butadiene–styrene copolymer with stainless steel fiber. Its physical properties and electromagnetic shielding effectiveness are tested. When the mass percent of stainless steel fiber is 15%, shielding effectiveness of composite is 21–59 dB in frequency band of 15 MHz to 3 GHz and cylindrical shell is made of it. Experiments under radiation of X-band high power microwave and ultra-wideband electromagnetic pulse are conducted in microwave anechoic chamber while magnetic fuzes connected with electrical fire head are placed at the center of cylindrical shell. Results show good agreement with test. Coupling effect is analyzed while shell has a hole or slot of millimeter level.

Keywords

Stainless steel fiber, acrylonitrile–butadiene–styrene copolymer, electromagnetic shielding, magnetic fuse, shielding effectiveness

Introduction

Stainless steel fiber (SSF) filled polymer composite is quite a useful kind of electromagnetic shielding materials, as it has good electromagnetic shielding effectiveness within a broad frequency range.[1–7] Besides its utility in civilian products against electromagnetic interference, it can also be used in military equipments to cope with electromagnetic warfare and electromagnetic radiation weapons on modern battlefield. This paper is attended to the latter.

SSF is a kind of conductive fiber filler which has been developed since 1980s.[8–11] It has excellent conductive property and processing property, especially that there is little oxidation on the surface in high temperature process. SSF-filled polymer composites exhibit percolation effect obviously and have preferable conductive property when SSF content is more than 10%. On the other hand, SSF filler has small influence on physical and mechanical properties of acrylonitrile–butadiene–styrene (ABS) copolymer compared with other fillers. SSF-filled ABS copolymer composite is practical and will have a good applied foreground. [12–16]

Composite preparation

Materials

SSF: Type AISI 316 L, diameter 10–13 μm, length 0.6–1 mm (Hunan Huitong Material Co., Ltd.); ABS: Type CB1230 (Shanghai Pret Composites Co., Ltd.); Ethylene acrylate copolymer, Silane coupling agent: Type KH-560, KH-570 (Du Pont China Holding Co., Ltd.); Decabromodiphenyl ether, Antimony trioxide (Chemtura Corporation).

There is an obvious difference between surface property of SSF and one of ABS matrix, and the crux of composite material preparation process is surface

[1]College of Field Engineering, PLA University of Science and Technology, Nanjing, Jiangsu, China
[2]College of Basic Education for Commanding Officers, National University of Defense Technology, Changsha, Hunan, China

Corresponding author:
Xian-nan Luo, College of Field Engineering, PLA University of Science and Technology, Nanjing 210007, Jiangsu, China.
Email: 13813802722@163.com

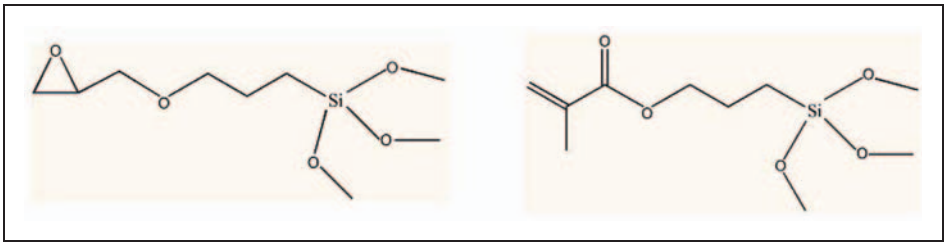

Figure 1. Chemical structure of $C_9H_{20}O_5Si$ and $C_{10}H_{20}O_5Si$.

treatments of SSF in order to form homogeneous mixture. The molecular structure of coupling agent includes lipophilic groups and hydrophilic groups, which has coupling with the ABS matrix and SSF filler respectively. Coupling agents minimize voids and help enhance mechanical properties. After surface modification, the resistivity of composite decreased significantly, while physical and mechanical properties have small difference with ABS copolymer.[17]

Chemical structure of silane coupling agent can be abbreviated as $YSiX_3$, in which Y and X represent lipophilic group and hydrolysable group, respectively. Molecular structure of type KH-560 is $C_9H_{20}O_5Si$, and it is $C_{10}H_{20}O_5Si$ for type KH-570. As shown in Figure 1, hydrolysable group is $–O–CH_3$ and lipophilic groups are $CH_2–CH(O)–CH_2–O–(CH_2)_3–$ and $CH_2–C(CH_3)–C(O)–O–(CH_2)_3$-. Loading percentage of two types of silane coupling agent is 0.25% for KH-560 and 0.5% for KH-570 in weight. There is a deposition process of 24 h at 25°C after the surface modification and 15 min of baking at 120°C before the mix manufacture.

Manufacture

Equipment: Single-screw extruder, type SJ-30, cutter (Nanjing Giant Machinery Co., Ltd.); Injection molding machine: Type HTB110X/1 (Ningbo Haitian Plastic Machine Co. Ltd.).

A special design of V-shape pouring mold is add to the single-screw extruder as self-design modification. The traction speed and adulterant added is controlled. SSF filler and ABS copolymer are melted and extruded in granulator, then cut to pellets of 8–11 mm in length, and finally made into a sample with injection mechanism.

Physical properties

Test instrument: Gap system prototype, type XQZ-1; Impact testing machine: Type XJC-25ZD (Chengde Precision Test Instrument Co., Ltd.). Electronic tensile machine: Type 4045; Digital micro ohm resistance measure: Type SW-2. (10^{-3}–$10^{3}\Omega$, Suzhou second radio factory). Surface resistance tester: Type 385 (10^{3}–$10^{12}\Omega$); Digital multimeter: Type DT-830. (10^{2} ~$10^{6}\Omega$) (NEC Corporation).

Test standard: Tensile properties test, ISO527-1993(E), tensile rate: 50 mm/min. Bending properties test: ISO178-1993(E), bending rate: 2 mm/min. Notched Izod impact strength test: ISO180-1993(E), temperature 23°C, the thickness of the sample is 3.21 mm, pendulum energy is 1 J. Thermal deformation temperature test: ISO75-1993(E), the thickness of sample is 6.4 mm; load pressure is 1.85 MPa, heating rate of 10°C/min. Surface resistivity and volume resistivity test: ASTM D257-92.

Table 1 shows physical properties of composite material.

Electromagnetic shielding effectiveness

Composite is prepared when the mass fraction of SSF is 15%. Testing sample size is $300 \times 300 \times 3.5\,mm^3$. Tests are conducted in welded steel shielding chamber according to national standard GB12190-2006 "electromagnetic shielding effectiveness measurement method". Reference standard is American military standard Mil-DTL-83528C.

There is a test window with a size of $600 \times 600\,mm^2$ in the welded steel shielding chamber, as shown in Figure 2.

Firstly, plug the window completely with steel plate, whose size is $720 \times 720 \times 2\,mm^3$. Fill the overlap with conductive gasket. Measure the power value of electromagnetic field at the center of the window. Define it as A.

Secondly, cut a square opening of $275 \times 275\,mm^2$ in the middle of steel plate. Measure the power value of electromagnetic field at the center of the window. Define it as B.

Finally, plug the square opening with sample. Fill the overlap with conductive gasket. Measure the power value of electromagnetic field at the center of the window. Define it as C. Electromagnetic shielding effectiveness of composite can be calculated by subtracting C from B.

SE is calculated by

$$SE = 10\lg(P_0/P_1) \quad (1)$$

Table 1. Physical properties of composites.

		SSF-filled ABS composites (mass fraction of SSF (%))		
Physical properties	ABS	10	15	25
Density (g/cm^3)	1.13	1.37	1.46	1.58
Tensile strength (MPa)	53.0	87.2	88.4	90.3
Bending strength (MPa)	87.6	83.9	80.7	71.4
Bending elastic modulus (MPa)	2250	2473	2570	3185
Impact strength (kJ/m^2)	59	47	43	35
Distortion temperature (°C)	102	115	117	121
Surface resistance (Ω)	10^{15}	1281.63	251.37	52.79
Volume resistance (Ω·cm)	10^{12}	967.14	410.72	182.57
Processing difficulty		Easy	Medium	Hard

ABS: acrylonitrile–butadiene–styrene; SSF: stainless steel fiber.

Figure 2. Electromagnetic shielding chamber.

where SE is the shielding effectiveness (dB); P_0, the received power (without composite material); P_1, the received power (with composite material).

Table 2 shows the electromagnetic SE of composite.

As a reference, SE of steel plate can be calculated by subtracting B from A. It is 42 dB, 40 dB, 55 dB, 70 dB, and 62 dB for 15 MHz, 100 MHz, 450 MHz, 950 MHz, and 3000 MHz, respectively. It can be concluded that composite material has a good SE of 21–59 dB linearly ascending from 15 MHz to 3 GHz, and the SE difference between it and standard material (steel) is less than 4 dB when the frequency is more than 100 MHz. After the test of physical properties and electromagnetic shielding effectiveness, composite should be tested in simulated battlefield electromagnetic environment.

Cylindrical shells are made in size of 115 mm diameter, 125 mm height, and 2 mm thickness. The bottom surface of shell can be split from the upper part of cylinder by thread connection with good sealing performance, as shown in Figure 3.

Table 2. Test value of SE (dB).

	Frequency (MHz)				
Value	15	100	450	950	3000
A	−65	−95	−47	−78	−65
B	−23	−55	8	−9	−3
C	−44	−93	−43	−65	−62
SE	21	38	51	56	59

SE: shielding effectiveness.

X-band high power microwave radiation effect experiments

X-band microwave source

X-band microwave source is composed of high frequency oscillator and modulator (Figure 4). It generates electromagnetic pulse with a certain repetition frequency and pulse width, which radiates through high frequency system.

Pulse generator is under the control of protective circuit. It generates a regulator triggered pulse. After regulator amplifier, the output pulse amplitude is about 800–950 V and pulse width is 0.5 μs or 1 μs. After modulator, the amplitude is about 34 kV and the modulated pulse is sent to the magnetron which generates high frequency pulse. Pulse repetition frequency depends on the pulse generator, and it can be divided into five levels.

Operating frequency is 9370 MHz (±100 MHz). Output pulse power is more than 200 kW. Pulse width

is 0.5 μs (±0.1 μs) or 1.0 μs (±0.1 μs). Pulse repetition frequency is 50 Hz, 100 Hz, 500 Hz, 1000 Hz or 2000 Hz. Duty ratio is less than 0.1%.

Experimental procedure

Microwave anechoic chamber's area is 12×8 m^2 and its height is 6 m. On inner surface of chamber there is carbon powder filled polyurethane-absorbing material. Experiment design is shown in Figure 5.

Step 1: Connect microwave source with transmitting antenna. Magnetic fuzes connected with electrical fire head are put on the table whose height is adjustable. Set the circuit board horizontal and make its height the same with the center of horn.

Step 2: Turn on power switch and control radiation for a certain period of time (60 s). Turn off microwave source. Unscrew the bottom surface and observe whether the fuze is triggered. If not obvious, detect electrical level of circuit board to find out whether it could still work.

Step 3: Magnetic fuzes connected with electrical fire head are set under composite shell put upright on the table. Set the circuit board horizontal and make its height the same with the center of horn (Figure 6). Repeat step 2.

Figure 3. Composite shell.

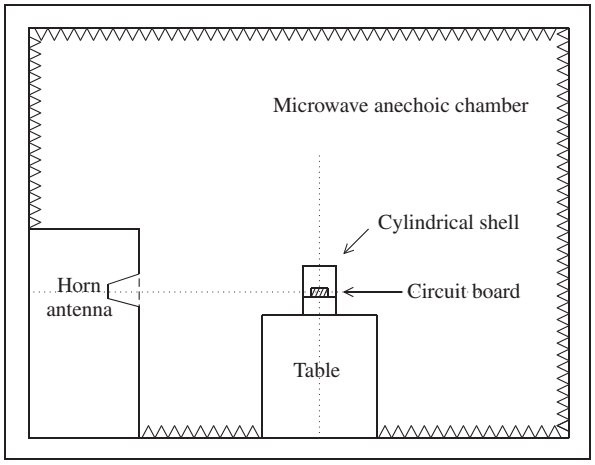

Figure 5. Experiment design.

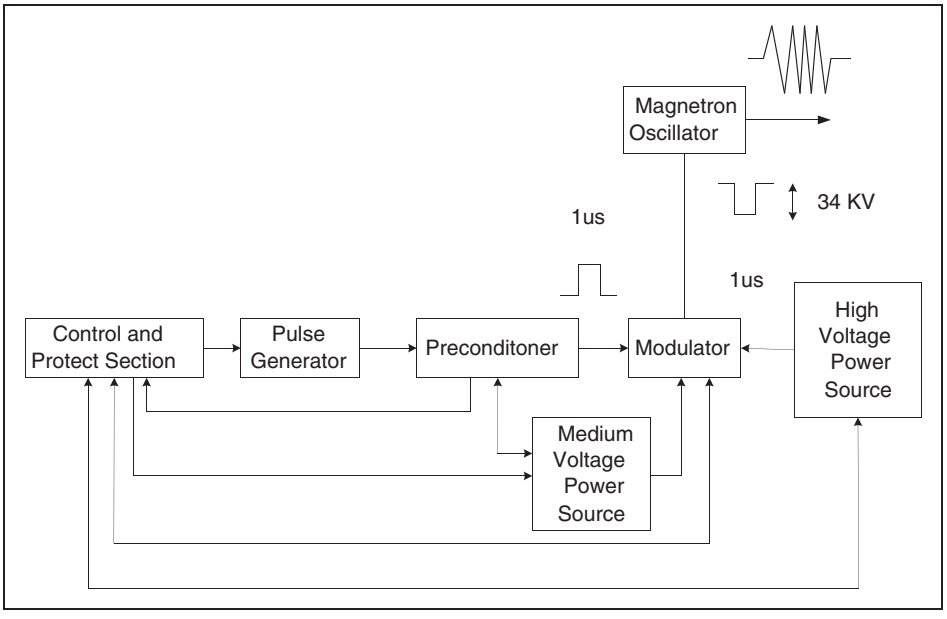

Figure 4. Components of microwave source.

Finally, change the direction of microwave polarization, pulse width, repetition frequency and the distance between placed position and horn antenna, repeat the above steps and record the data.

Experiment results

Horn antenna aperture has a size of $135 \times 104\,\text{mm}^2$. Antenna gain is about 20 dB.

Wavelength (λ) is 32.0 mm on working frequency, which is much more less than the length of antenna aperture. As electrically large antenna, according to the division of antenna field region, the lower bound of the far field region is

$$r_f = \frac{2L^2}{\lambda} \tag{2}$$

where L is 135 mm and the lower bound is 1139 mm.

Calculation method of electric field intensity on measure point is different depends on whether the point is in far-field region or near-field region.

When circuit board is placed in far-field region, power value of electromagnetic field can be obtained by

$$P = \frac{P_t}{4\pi R^2} G \tag{3}$$

where P_t is the transmitting power of antenna (200 kW), G represents antenna gain, and R is the distance between antenna aperture and measure point.

The average Poynting vector is

$$P = \frac{1}{2}\text{Re}(E \times H^*) \tag{4}$$

Impedance of free space wave Z_0 (equals to E/H^*) is 377 Ω. Then the electric field intensity could be calculated by equations (3) and (4).

When circuit board is placed in near-field region, electric field intensity can be calculated by

$$E_r = E_a A_e/(R\lambda) \tag{5}$$

where E_r represents electric field intensity of measure point, E_a is the electric field intensity on horn surface, and A_e represents effective aperture.

$$A_e = \frac{7.5}{4\pi} wh \tag{6}$$

Here W and h represent width and height of horn aperture, respectively.

$$P = \frac{E_a^2}{Z_0} A_e \tag{7}$$

P is the transmitting power of horn antenna. Then the electric field strength values can be calculated.

Shell is airtight, thus field strength meter probe cannot be placed in it. Electric field intensity value inside shell can be obtained through numerical calculation method (Ansoft HFSS software). The calculation model is shown in Figure 7. Perfectly matched layer (PML) absorbing boundary condition is adopted.

When magnetic-acoustic fuze and magnetic-vibrational fuze are placed parallel to the polarization direction of microwave source, electric field intensity of center point of circuit board is calculated, no matter whether there is a composite shell or not. Nine groups of data in both cases are selected and shown in Tables 3 and 4.

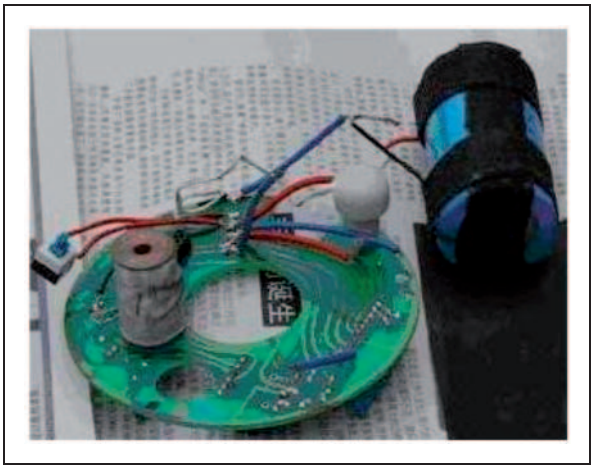

Figure 6. Circuit board.

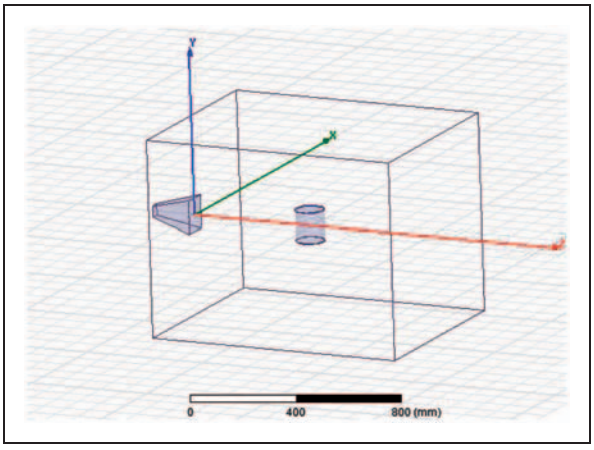

Figure 7. Calculation model.

Table 3. Experiment results of magnetic-acoustic fuze (horizontal polarization).

Pulse width (μs)	Repeat frequency (Hz)	Distance (m)	Without shell (V/cm)		With shell (V/cm)	
1	100	1.5	A	230.9	A	5.54
1	500	1.5	B	230.9	A	4.56
0.5	2000	1.5	B	230.9	A	3.87
1	100	0.5	B	499.2	A	12.0
1	500	0.5	B	499.2	A	9.86
0.5	2000	0.5	C	499.2	A	8.36
1	100	0.2	C	1248	A	30.0
1	500	0.2	C	1248	A	24.7
0.5	2000	0.2	D	1248	A	20.9

Table 4. Experiment results of magnetic-vibrational fuze (horizontal polarization).

Pulse width (μs)	Repeat frequency (Hz)	Distance (m)	Without shell (V/cm)		With shell (V/cm)	
1	100	0.6	A	451.3	A	10.8
1	500	0.6	A	451.3	A	8.91
0.5	2000	0.6	A	451.3	A	7.56
1	100	0.4	A	679.6	A	16.3
1	500	0.4	B	679.6	A	13.4
0.5	2000	0.4	B	679.6	A	11.4
1	100	0.2	C	1316	A	31.6
1	500	0.2	C	1316	A	26.0
0.5	2000	0.2	D	1316	A	22.1

A: fuze is normal after detection; B: short time invalidation (there is logic confusion in immediate detection but detection again after 5 min shows it has returned to normal); C: long time invalidation (there is logic confusion in immediate detection and detection again after 30 min shows it is still abnormal); D: complete damaged (electrical fire head is ignited).

Data in the table show that electric field strength to completely damage magnetic-acoustic fuze is about 1250 V/cm, and 1300 V/cm for magnetic-vibrational fuze. Threshold of 50% failure probability is 500 V/cm and 700 V/cm for each one.

Shielding effectiveness of different conditions is shown in Figure 8. In this experiment, the test of composite shell under X-band HPM radiation shows that its SE is more than 20 dB. SE on low pulse repetition frequency is less than that on high pulse repetition frequency.

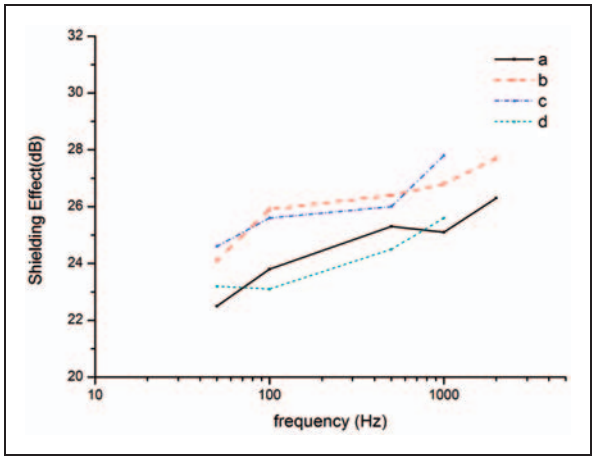

Figure 8. Shielding effectiveness of composite shell. a: pulse width is 0.5 μs and polarization direction is horizontal; b: pulse width is 0.5 μs and polarization direction is vertical; c: pulse width is 1 μs and polarization direction is horizontal; d: pulse width is 1 μs and polarization direction is vertical.

Slot coupling effect

When there is a hole or slot on composite shell, it will engender electromagnetic leakage and coupling effect.

A set of 20 samples are tested after drilling and cutting operation. Radius of circular hole decreases from 9 mm to 4 mm (1 mm each step). Cross-section width of rectangular slot is 1 mm and length decreases from 30 mm to 4 mm (2 mm each step). Thickness of shells is 2 mm. Holes and slots are in position of half shell height.

Table 5. SE of different shells (dB).

SE(dB)		Intact shell	Shell with a circular hole (Radius of circle)				Shell with a rectangular hole (Length of rectangle)				
			9 mm	7 mm	5 mm	4 mm	30 mm	22 mm	16 mm	10 mm	4 mm
Verticalpolarization	0.5 μs	25.1	14.1	16.4	24.6	25.0	15.9	16.0	14.1	22.6	24.5
	1 μs	27.8	15.6	16.3	25.4	26.9	16.1	16.3	14.2	22.9	25.3
Horizontal polarization	0.5 μs	26.8	14.7	17.5	25.7	26.3	16.2	17.2	14.5	23.4	25.0
	1 μs	25.6	16.2	17.1	24.8	25.2	16.6	18.8	14.7	23.2	24.6

SE: shielding effectiveness.

Conduct the same experiment in section 3.3. When the distance between circuit board and horn antenna is 1 m and pulse repetition frequency is 1000 Hz, nine groups of data is selected and shown in Table 5.

Wavelength (λ) is 32.0 mm on operating frequency. When the radius decreases from 9 mm to 5 mm, SE gradually increases. Main influencing factor is the radius and the angle between polarization direction and shell midline has small influence. When the radius is less than 5 mm, the difference of SE between shell with a circular hole and intact shell is less than 1.0 dB and radius tends to have no influence on SE.

When the rectangular length decreases from 30 mm to 10 mm, SE gradually rises. Angle between polarization direction and slot has influence on SE. SE of horizontal polarization is better than SE of vertical polarization. When the slot length is less than 10 mm, SE is gradually close to the one of intact shell. However, when the aperture length is 16 mm, the SE has a reduction of about 2–4 dB, which is different from the rising trend. For this situation the ratio l/λ is 1/2, and there is resonance occurring as coupling effect on slot.

Ultra-wideband pulse radiation effect experiments

Ultra-wideband electromagnetic pulse source

Pulse source has a switch voltage of 280 kV and peak power of 1 GW. Attenuation from source to oscillograph is 40 dB. Pulse repetition frequency is 1 Hz, 5 Hz, 10 Hz, 20 Hz, or 50 Hz and pulse width is about 2.5 ns. Radiation efficiency of axis direction of transverse electromagnetic (TEM) antenna is about 35% (Figure 9).

Measuring antenna of pulse radiation field is 60 cm long TEM horn antenna with sensitivity of 2.8 cm. Radiation field can be estimated by

$$E = U/(S \times A) \tag{8}$$

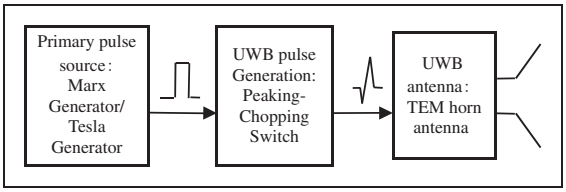

Figure 9. Pulse generator.
UWB: ultra-wideband.

where E is electric field strength (V/cm); U is the voltage shown on oscillograph (V); S is the sensitivity of measuring antenna (2.8 cm).

A is a S_{21} parameter of coaxial cable transmission line and has no dimension. In 10 MHz to 2 GHz frequency range, its value depends on cable type. (1) 20 m SVY50-9 cable and 2 m SVY50-5 cable, $A = 0.70$; (2) 100 m SVY50-9 cable and 2 m SVY50-5 cable, $A = 0.21$.

Experimental procedure

Experiment is conducted in three steps (Figure 10).

Step 1: Connect pulse source with ultra-wideband (UWB) antenna. Composite shell is placed upright and the bottom surface is 0.8 m high from ground. Magnetic fuzes connected with electrical fire head are set in it. Circuit board is put horizontal and in the same height with the center of horn.

Step 2: Turn on power switch and control radiation for a certain period of time (60 s). Turn off pulse source. Unscrew the bottom surface and observe whether the fuze is triggered. If not obvious, detect electrical level of circuit board to find out whether it could still work.

Step 3: Change pulse repetition frequency or the distance between placed position and pulse source, repeat the above steps and record data.

Shielding effectiveness calculation

Shielding effectiveness of composite shell can be calculated by numerical simulation method whether shell is intact or with a hole.

Pulse source is approximated by differential Gauss pulse

$$E(t) = E_0 k(t - t_0) \exp\left(-\frac{4(t - t_0)^2}{\tau^2}\right) \quad (9)$$

where $k = \frac{\sqrt{8\pi e}}{\tau}$, τ is the pulse width, t_0 is delay time and pulse rise time is about $\tau/4$. According to the characteristics of radiation antenna, pulse radiation E_0 is 40 kV/m, τ is 2 ns and the pulse radiation source is approximated by plane wave radiation.

Simulation model. This model is a cylinder with diameter of 115 mm, height of 125 mm, and thickness of 2.5 mm. Electromagnetic parameters of composite shell are set as follows: conductivity is 2.43×10^{-3} S/m. Relative permittivity is 3.5 and relative permeability is 1.0. Two models are established by using CST software, as shown in Figure 11, considering whether there is a hole on shell or not. Cylinder is vertically suspended and the bottom surface is 0.8 m high from ground. Distance between TEM horn antenna aperture surface and cylinder center is 2.5 m, 1.0 m, 0.5 m, or 0.35 m. A probe is set in the point of cylinder center, and Ez value and SE are calculated.

Figure 10. Experiment design.

Model 1: Shell is intact and plane wave incidents perpendicular to shell.

Model 2: There is a circle hole on shell with a diameter of 7.0 mm, 6.0 mm, 5.0 mm, 4.5 mm, or 4.0 mm, and circle center is in half height of cylinder.

Calculation results. When shell is intact and distance is 0.5 m between shell and antenna, calculation of shielding effectiveness is shown in Figure 12.

Figure 12(a) is waveform of incident UWB pulse. Figure 12(b) shows energy distribution of incident pulse in frequency domain after fast Fourier transform. Pulse energy is mainly distributed in the range of 10 MHz to 2 GHz. Figure 12(c) is voltage waveform of point of cylinder center. By comparing peak value of electric field in Figure 12(a) and (c), shielding effectiveness is calculated as shown in Figure 12(d), which is transformed from time domain to frequency domain.

As shown in Figure 12, SE of composite shell under UWB electromagnetic pulse radiation is more than 25 dB. Using the same method, SE of shell with a circle hole can be calculated and the results are shown in Table 6.

Data analysis

It can be summarized by analyzing data:

1. Electric field inside shell has an oscillation after incident pulse. As shown in Figure 11(c), oscillating period is about 2.2 ns, and resonant frequency is about 455 MHz. Thus, working frequency of circuit components should not in the vicinity of resonant frequency, in which coupling effect exists.

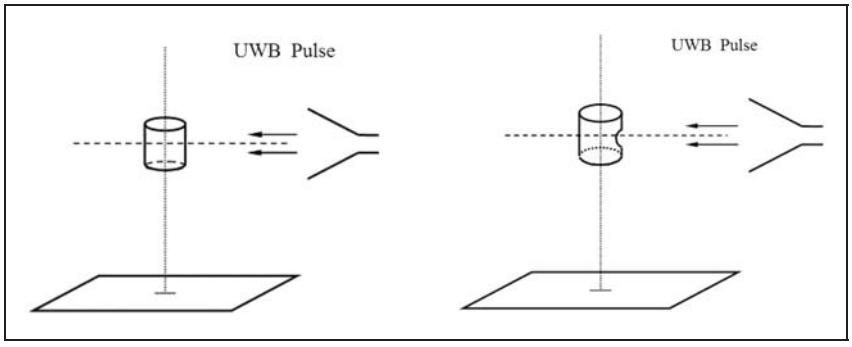

Figure 11. Calculation models.
UWB: ultra-wideband.

2. UWB electromagnetic pulse can easily pass through opening into interior. Stationary wave is formed in the cavity after reflection and refraction. Circuit components located in antinodes are in high energy density of electromagnetic field, what should be avoided if possible.

Radiation field E on a certain distance can be calculated using equation (8). Calculation data when the pulse repetition frequency is 20 Hz is shown in Table 7.

Data shows that threshold of fuze failure is about 25 kV/m. When the distance between composite shell and UWB antenna is more than 0.5 m, the inner fuze can work normally on condition of that incident pulse has peak power of 1 GW.

A circular hole is drilled on a set of five samples. Diameter is distributed as 7.0 mm, 6.0 mm, 5.0 mm, 4.5 mm, and 4.0 mm. Experimental steps are repeated in section 4.2. When distance between shell and antenna is 0.5 m and pulse repetition frequency is 20 Hz, experiment results are showed in Table 8.

It can be concluded from Table 8 that when the cylindrical shell has only single hole with diameter less than 4.5 mm, its influence on SE is less than 0.5 dB.

Table 6. SE calculation (dB).

Distance		2.5 m	1.0 m	0.5 m	0.35 m
Intact shell		26.7	26.1	25.3	24.6
Circle diameter (mm)	4.0	26.6	25.9	25.0	24.4
	4.5	26.4	25.7	24.8	24.1
	5.0	26.1	25.2	24.3	23.5
	6.0	25.4	24.5	23.6	22.8
	7.0	24.6	23.6	22.5	21.6

SE: shielding effectiveness.

Table 7. Experiment result.

Distance (m)	Indicator (V)	Electric field (kV/m)	Result
2.5	0.62	3.16	In good condition
1.0	1.48	7.55	In good condition
0.50	3.0	15.3	In good condition
0.35	4.9	25.0	Logical confusion

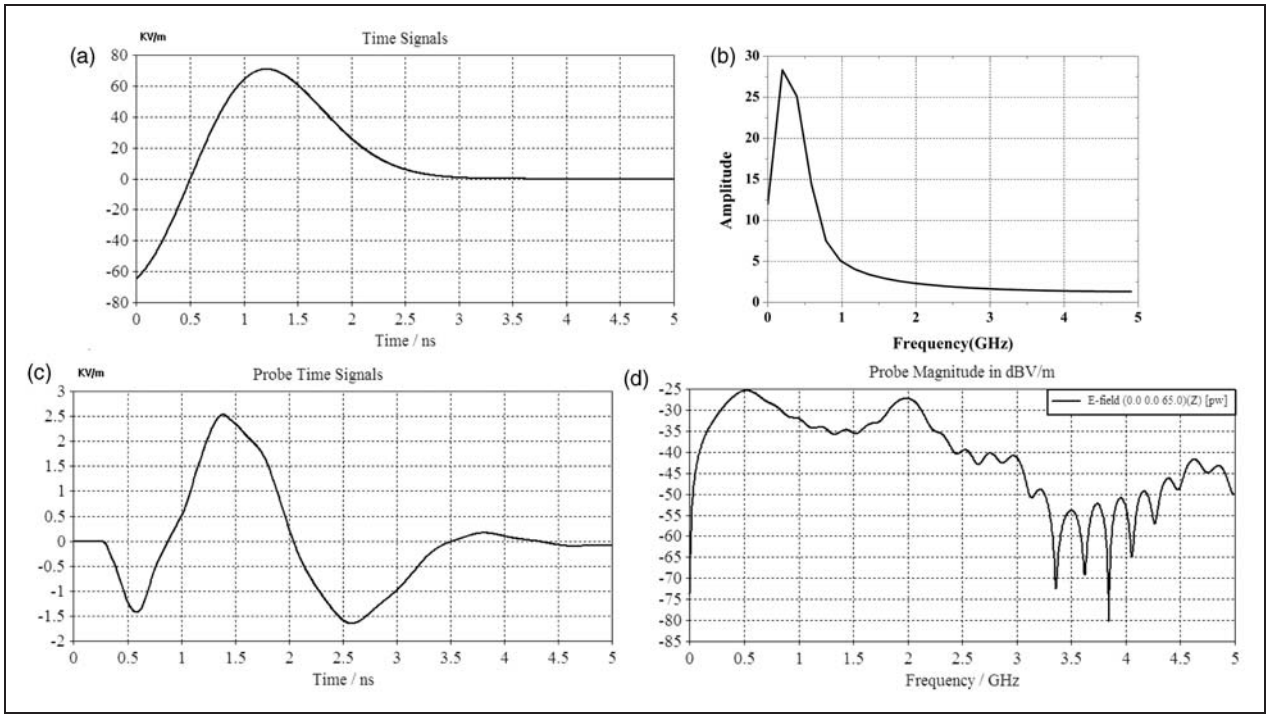

Figure 12. Shielding effectiveness calculation: (a) electric field waveform of pulse; (b) energy distribution in frequency domain; (c) electric field waveform of probe; (d) shielding effectiveness.

Table 8. SE of shells with a circular hole.

Diameter (mm)	Indicator (V)	Electric field (kV/m)	Result
4.0	3.0	15.3	In good condition
4.5	3.1	15.7	In good condition
5.0	3.3	16.6	In good condition
6.0	3.5	18.0	In good condition
7.0	4.0	20.4	In good condition

SE: shielding effectiveness.

Conclusions

1. Filling ABS copolymer with stainless steel fiber is an effective method to prepare electromagnetic shielding material. When the mass percent of SSF is 15%, shielding effectiveness of composite is 21–59 dB in frequency band of 15 MHz to 3 GHz.
2. Cylindrical shells made of composite exhibit good shielding effect under radiation of X-band high power microwave (HPM) source and UWB electromagnetic pulse source. Only when the distance between shell and source is less than 0.2 m or 0.5 m respectively can magnetic fuzes connected with electrical fire head placed in it be triggered.
3. If shell has a rectangular slot of millimeter level which is comparable to wavelength of incident radiation, shielding effectiveness gradually rises as rectangular length decreases. However, shielding effectiveness has a reduction of about 2–4 dB when the ratio of slot length compared with wavelength is 1/2 because there is resonance happened as coupling effect on slot. When the ratio is less than 1/3, shielding effectiveness is gradually close to the one of intact shell.
4. If shell has a circular hole of millimeter level which is comparable to wavelength of incident radiation, shielding effectiveness gradually rises as radius decreases. The difference of shielding effectiveness between intact shell and it is less than 1.0 dB when the radius is less than 5 mm under radiation of X-band HPM source. For situation of UWB electromagnetic pulse source, when the diameter is less than 4.5 mm, the difference is less than 0.5 dB.

Acknowledgments

The authors are thankful to the State Key Lab of Disaster Prevention and Mitigation of Explosion and Impact for material testing equipment and the National Defense Science and Technology Key Lab for Electromagnetic Environment Effects and Electrooptical Engineering for experimental facilities.

Funding

This research received no specific grant from any funding agency in the public, commercial, or not-for-profit sectors.

Conflict of interest

None declared.

References

1. Tan ST, Zhang MQ, Rong MZ, et al. Interfacial interaction in stainless steel fiber-filled polypropylene composites. *J Appl Polym Sci* 2000; 78: 2174–2179.
2. Notingher PV, Panaitescu D, Paven H, et al. Some characteristics of conductive polymer composites containing stainless steel fibers. *J Optoelectron Adv Mater* 2004; 6: 1081–1084.
3. Chen HC, Lin JH and Lee KC. Electromagnetic shielding effectiveness of copper/stainless steel/polyamide fiber cowoven-knitted fabric reinforced polypropylene composites. *J Reinf Plast Compos* 2008; 27: 187–204.
4. Wu HH, Sun XZ and Cai GY. A study of the layered microstructure and electrical resistivity of an injection-molded metallic fiber-filled polymer composites. *Polym J* 2012; 44: 1138–1144.
5. Chen X, Chen YG and Wei M. Model for clipping-induced timing error of bandwidth-limited comparators. *Electron Lett* 2013; 49: 531–532.
6. Fox RT, Wani V, Howard KE, et al. Conductive polymer composite materials and their utility in electromagnetic shielding applications. *J Appl Polym Sci* 2008; 107: 2558–2566.
7. Chen CS, Chen WR, Chen SC, et al. Optimum Injection Molding Processing Condition on Electromagnetic Interference Shielding Effectiveness of Stainless Steel Fiber Filled Polycarbonate Composite. *Int Commun Heat Mass Transfer* 2008; 35: 744–749.
8. Lundgren U, Ekman J and Delsing JT. Shielding effectiveness data on commercial thermoplastic materials. *IEEE Trans Electromagn Compat* 2006; 48: 766–773.
9. Wu JH and Chung D. Pastes for electromagnetic interference shielding. *J Electron Mater* 2005; 34: 1255–1258.
10. Li L and Chung D. Electrical and mechanical properties of electrically conductive polyethersulfone *composites*. *Composites* 1994; 25: 215–224.
11. Tan ST, Zhang MQ, Rong MZ, et al. Properties of metal fibre filled thermoplastics as candidates for electromagnetic interference shielding. *Polym Polym Compos* 2001; 9: 257–262.
12. Yang SY, Chen CY and Parng SH. Effects of conductive fibers and processing conditions on the electromagnetic shielding effectiveness of injection molded composites. *Polym Compos* 2002; 23: 1003–1013.
13. Kim MS, Kim HK, Byun SW, et al. PET fabric/polypyrrole composite with high electrical conductivity for EMI shielding. *Synth Metals* 2002; 126: 233–237.
14. Wen SH and Chung D. Electromagnetic interference shielding reaching 70 dB in steel fiber cement. *Cem Concr Res* 2004; 34: 329–332.

15. Lin JH, Lou CW, Lu CK, et al. Functional fabric of hybrid stainless steel/polypropylene and the electrical properties of thermoplastic composites. *J Adv Mater* 2004; 36: 63–68.
16. Chen SC, Chien RD, Lee PH, et al. Effects of molding conditions on the electromagnetic interference performance of conductive ABS parts. *J Appl Polym Sci* 2005; 98: 1072–1080.
17. Park DH, Lee YK, Park SS, et al. Effects of hybrid fillers on the electrical conductivity and EMI shielding efficiency of polypropylene/conductive filler composites. *Macromol Res* 2013; 21: 905–910.